JOURNAL OF MATERIALS SCIENCE 30 (1995) 2722–2728

A new theory to obtain Weibull fibre strength parameters from a single-fibre composite test

K. GODA
Department of Mechanical Engineering, Hiroshima University, Higashi-Hiroshima, 724, Japan

J. M. PARK
Department of Polymer Science and Engineering, Gyeongsang National University, Chinju, Korea

A. N. NETRAVALI
Fibre Science Program, Department of Textiles and Apparel, Cornell University, Ithaca, NY 14853, USA

A theory is developed to obtain the Weibull scale and shape parameters for *in situ* fibre strength utilizing the data obtained from a single-fibre-composite (SFC) test. It is well known that during the SFC test, the fibre fractures several times along its length at successive weak points that are randomly located. The SFC technique, although most commonly used for measuring the fibre/matrix interfacial shear strength, is an excellent way to determine the fibre flaw spacings and the *in situ* fibre failure stress at every fracture location. In the present technique, the SFC specimen is partitioned into a relatively large number of small sections of equal length such that each section will have either one or no fibre fracture point. Because all the sections may not include the fibre fracture points because of their random nature, the test data are regarded as "censored data". In other words, the theory is constructed for the estimation of Weibull parameters that takes into account the censored nature of the data. The Weibull parameters predicted using the present theory are in the same range as those obtained from the single fibre tension tests. For several reasons the values obtained from the SFC test tend to be slightly higher than those obtained from the simple tension tests. However, the *in situ* fibre strength values obtained using SFC technique may be more realistic and thus may be more useful in modelling composite strength.

1. Introduction

Advanced polymeric composites that utilize high-performance fibres are being routinely used in place of more conventional metals and metallic alloys in military and commercial aerospace applications. The popularity of these lightweight and high-strength composites is now spreading fast into a variety of other applications from sports gear to automotive parts. The mechanical properties of these composites are basically derived from the fibre strength, matrix properties and the fibre/matrix interfacial strength. While the measurement of fibre strength and matrix properties are fairly simple, measuring *in situ* fibre strength, which is critical in modelling strength of composite materials, is not so straightforward.

Measuring fibre/matrix interfacial strength requires special techniques. Some of the most commonly used techniques include the single-fibre composite (SFC) test [1–8], single-fibre pull-out [9, 10], and microbonding [11]. A modified single-fibre pull-out from a microcomposite has also been recently developed [12]. The SFC test, the topic of this paper, has been shown to yield quantitative information about the interfacial shear strength as well as the interfacial failure mode. Recently, the SFC test has also been used to measure *in situ* fibre strength [13–16].

The SFC test is a straightforward procedure in which a single fibre is embedded along the centre line of a relatively large dog-bone shaped specimen of matrix material and then straining the specimen uniaxially along the fibre (and the specimen) axis [3]. As the specimen is strained, the shear in the matrix puts a tensile load on the fibre through the fibre/matrix interface. At some strain, the tensile stress in the fibre matches the fibre fracture stress at the weakest flaw within the gauge length and the fibre breaks at that flaw. The fractured ends of the fibres do not carry any load but the stress builds up linearly away from the break, provided that the fibre/matrix interface does not fail. The length over which the stress builds up to the maximum, is called as the stress recovery region or the ineffective length. However, if the interface fails, i.e. if the fibre debonds over a length, the stress recovery region is bilinear [17]. The first part, with a lower slope, is due to the fibre/matrix friction in the debonded region and the other part,

0022–2461

with significantly higher slope, is due to the matrix shear. The specimen, generally having a higher strain to failure than the fibre, can be further strained. With increasing specimen strain, the stress on the fibre increases and it breaks at the next weakest flaw location when the flaw strength equals the stress on the fibre. The fracture process continues and as a result, the fibre fractures at different flaw locations resulting in more fragments. At some point, the fragments become so short that the shear transfer along their lengths can no longer build up enough tensile stress to cause any further failures even with increasing strain [1–5]. The test at this point is complete and the resulting fragment length distribution is the raw data from the SFC test. Fragment lengths, for transparent matrix, can be determined directly using optical microscopy.

Based on the force balance in a micromechanical model, Kelly and Tyson [18, 19], showed that the maximum length of the fragment, l_c (also called the critical fragment length), is given by

$$l_c = d\sigma_f/2\tau \quad (1)$$

where d is the fibre diameter, σ_f is the fibre fracture stress, and τ is the yield stress in shear of the matrix or the interface. Some authors have assumed a uniform fragment length distribution with a mean l, of 0.75 l_c [7]. Henstenburg and Phoenix [17] have developed a refined model of the fragmentation process based on the Poisson/Weibull flaws along the fibre length and a linear buildup of the fibre tensile stress away from the fibre fracture locations. They developed a relationship which facilitated the formulation of the model as a Monte Carlo simulation problem in terms of a single factor, the Weibull shape parameter, ρ, for fibre strength. Along with simulating the non-dimensional fibre fragment length distribution, they showed that

$$\tau = (d\sigma_l/2l)(\Lambda_\rho/2)^{(\rho+1)/\rho} \quad (2)$$

where σ_l is the Weibull scale parameter for the fibre strength at a gauge length equal to the mean fragment length, l. The quantity Λ_ρ is the non-dimensional mean aspect ratio (l/h), where h is a certain characteristic length which is also derived from their model. The factor $(\Lambda_\rho/2)^{(\rho+1)/\rho}$ varies between 0.67 for very large ρ, to 0.97 for $\rho = 3$.

An exact theory of fragmentation describing the evolution of fibre fragmentation as a function of the underlying statistical strength of the fibre and the interfacial strength has been developed by Curtin [8]. Predictions of the theory when compared with the computer simulations of fibre fragmentation for several common models of stress recovery around fibre breaks showed excellent agreement. The theory could also be used to derive the *in situ* fibre strength.

Fibre diameter, d, in Equations 1 and 2 may be determined optically or using the vibroscope technique [3]. Because testing the fibre at very short gauge lengths of the order of l is impossible in most cases, the value of σ_l is obtained by tensile testing a number of fibre specimens at several convenient gauge lengths and then using the "Weibull weakest link rule" (size effect) [20]. However, for several reasons, this value of fibre strength obtained independently may differ from the *in situ* fibre strength.

Recently, there have been efforts to obtain fibre strength distribution and size effect from the SFC test itself [13–16]. Because the fibre fractures at successive weak points during the SFC test, this technique is an excellent way to determine the fibre flaw spacings and the *in situ* fibre failure stress at every fracture location within the test gauge length. Furthermore, the strength values obtained are for very short gauge lengths which cannot be obtained by conventional tension tests. If one assumes continuity of strain in the SFC specimen, one can obtain fibre fracture stress from the external, true stress applied on the SFC specimen, σ_a, using the relation given by

$$\sigma_f = \sigma_a E_f/E_m \quad (3)$$

where E_f and E_m are the fibre and matrix moduli, respectively, which can be obtained from independent tension tests. The validity of this approach was demonstrated earlier by Wagner and co-workers [13, 14]. Their apparatus consisted of a video camera to monitor the fibre break sequence and a load cell to measure the stress applied to the SFC specimen. They used a number of fibres including glass, graphite, and Kevlar fibres, in their study. Their results showed that the mean fragment length decreases with the applied stress, as expected, and that they could evaluate the fibre strength–length relationship. They were also able to obtain the Weibull shape and scale parameters for the fibre strength.

Sachse *et al.* [15] used the acoustic emission-coupled SFC (AE/SFC) test to locate the fibre fracture points and Equation 3 to compute the fibre failure stress. Their results showed that the *in situ* fibre strength values were higher than those obtained by the conventional tension tests. They argued that the higher strength values were mainly a result of the extended debond region along the fibre/matrix interface originating at the fibre fracture point, resulting in a smaller gauge length and possibly, bridging of the pre-existing cracks in the fibre by the epoxy matrix. However, the higher strength values in the SFC test may also be due to the fact that some of the severe flaws may be present in the stress recovery region and hence remain undetected. The data from the AE/SFC technique also showed a change in slope at a particular fragment length which indicated the possibility of different flaw populations for fibres longer and shorter than this length. Waterbury and Drzal [16] who also used the SFC test to estimate the fibre strength, obtained good correlation between the strength values obtained from the single-fibre tensile tests and *in situ* strength values from the SFC test. In this paper we present a new technique to evaluate the Weibull parameters for *in situ* fibre strength using the SFC fragmentation data.

2. Estimation of Weibull parameters for fibre strength

After completion of the SFC test, we consider, conceptually, partitioning the SFC specimen into a large

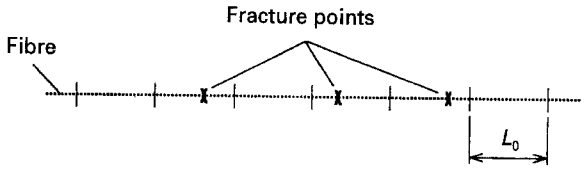

Figure 1 Schematic illustration of the partition into short sections.

number of N sections, each with length L_0, as shown in Fig. 1, which may or may not include a fibre fracture point. We assume the same result will be obtained as that of the SFC test, if we carry out the tensile test below a certain stress level after cutting the SFC specimen into N sections. For the sections which contain no fracture points, we assume that the fibre did not fracture, because the strength of those fibre sections were higher than the stress to which they were subjected. However, as mentioned earlier, the fibre may not break at some severe flaws because of their being in the stress recovery regions caused by a break on either side. The recovery regions can only occur after the fibre has broken at least once. This is an inherent property of the single-fibre composite test and reflects the actual situation in a composite loaded in tension. Hence, the fibre strength estimated from the SFC test may be of more practical significance than the values obtained from single-fibre tension tests.

Now, according to the assumption, we will obtain a random sample of r fibre strength values, i.e. $\sigma_1, \sigma_2, \ldots, \sigma_r$ where $\sigma_1 \leqslant \sigma_2 \leqslant \cdots \leqslant \sigma_r$, and the remaining $(N - r)$ specimens are unbroken, as conceptually mentioned above. This sample is called the "censored sample" for which the maximum likelihood estimation method may be used to estimate Weibull parameters, if we regard the fibre strength, σ_r, as the last censored datum [21]. The likelihood function, L, for the sample is generally given as follows:

$$L = \frac{N!}{(N-r)!} f(\sigma_1) f(\sigma_2) \cdots f(\sigma_r)[1 - F(\sigma_r)]^{N-r} \quad (4)$$

where $f(\sigma_i)$ is the probability density function of strength, σ_i, $i = 1, 2, \ldots, r$, and $F(\sigma)$ the cumulative distribution function. As used by other researchers, we can now apply the following two-parameter Weibull distribution to the functions $F(\sigma)$ and $f(\sigma)$ of Equation 4

$$F(\sigma) = 1 - \exp\left[-\frac{L}{L_0}\left(\frac{\sigma}{\sigma_0}\right)^m\right] \quad (5)$$

$$f(\sigma) = \frac{L}{L_0}\frac{m\sigma^{m-1}}{\sigma_0^m}\exp\left[-\frac{L}{L_0}\left(\frac{\sigma}{\sigma_0}\right)^m\right] \quad (6)$$

where m and σ_0 are the Weibull shape and scale parameters for fibre strength, respectively [22, 23]. L is the extrapolated gauge length to which the strength is scaled. L_0 is the original gauge length of individual sections in the partitioned SFC specimen as mentioned earlier. The least fragment length may be taken as L_0, because two or more fracture points can never be put in a single section of the specimen.

By making the log likelihood function $\ln L$, from Equation 4, and equating both $d\ln L/dm$ and $d\ln L/d\sigma_0$ to be zero, we obtain

$$\frac{1}{\hat{m}} + \frac{1}{r}\sum_{i=1}^{r}\ln\sigma_i - \frac{\sum_{i=1}^{r}\sigma_i^{\hat{m}}\ln\sigma_i + (N-r)\sigma_r^{\hat{m}}\ln\sigma_r}{\sum_{i=1}^{r}\sigma_i^{\hat{m}} + (N-r)\sigma_r^{\hat{m}}} = 0$$

$$\hat{\sigma}_0 = \left\{\frac{L_0}{L}\frac{1}{r}\left[\sum_{i=1}^{r}\sigma_i^{\hat{m}}\ln\sigma_i + (N-r)\sigma_r^{\hat{m}}\right]\right\}^{1/\hat{m}} \quad (7)$$

where $\hat{m}$ and $\hat{\sigma}_0$ are the estimators of m and σ_0, respectively. The first part of Equation 7 can be solved by the iterative technique such as the Newton–Raphson method. After obtaining the value of $\hat{m}$, $\hat{\sigma}_0$ can be calculated using the second part of Equation 7. In the present study, the Weibull parameters were estimated for 10 mm gauge length, using the above technique and compared with the results obtained by the single fibre tension tests.

3. Experimental procedure

The Nicalon™ fibre used was a ceramic grade silicon carbide fibre (15 μm nominal diameter) manufactured by Nippon Carbon Co. Ltd of Japan. The reported mass density of the fibre is 2.55 g cm^{-3}, the elastic modulus is between 176.4 and 196 GPa and average strength is 3000 MPa. Fibres without sizing were obtained in the form of a tow containing 500 filaments. After cutting about 250 mm long piece of the fibre tow, fibres were carefully extracted. To determine the linear density of each specimen, a piece about 60 mm long was cut from one end of the fibre and vibroscoped according to ASTM 1577-79. Using the linear density and the known mass density of 2.55 g cm^{-3}, the diameter of each fibre was calculated. The remaining part of the fibre was mounted on a paper tab using a quick-setting epoxy adhesive, with a gauge length of 10 mm, and tested on an Instron tensile testing machine (Model 1122) interfaced with a computer. All fibres were tension tested at a strain rate of 0.02 min^{-1} according to ASTM D3379. The tests were performed, under standard textile conditions of 20 °C and 65% relative humidity. Individual fibre fracture stress values were calculated from the diameter and the fracture load. To obtain the gauge length–strength (size) effect, fibres were also tested at gauge lengths of 200 mm. At least fifty single-fibre specimens were tested at each gauge length to obtain a statistical distribution. Data for 5 mm and 100 mm gauge lengths for the same Nicalon fibre were taken from another reference paper for comparison [15].

Epoxy resin DER 331 was blended with DER 732 and then mixed with curing agent DEH no. 26 in stoichiometric proportion. Both the resins and the curing agents were provided by Dow Chemical Company. DER 331 is a bisphenol-A (DGEBA)-based epoxy. DER 732 is a polyglycol diepoxide and is used as a flexibilizer. The curing agent DEH no. 26 is tetraethylenepentamine (TEPA).

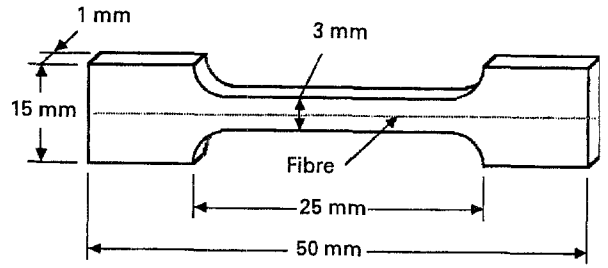

Figure 2 Dimensions of the single-fibre composite specimen.

Dog-bone shaped epoxy SFC specimens (Fig. 2) were fabricated in silicone rubber moulds [3]. The flexibilized epoxy resin was prepared by mixing DER 331 (80% by weight) and DER 732 (20%) and then adding the required amount of DEH 26. This proportion was chosen to obtain sufficient matrix fracture strain and to ensure that there is no matrix crack at the fibre fracture points [3]. After thoroughly stirring, the mixture was degassed to remove the air and poured into the mould containing a single Nicalon™ fibre suspended in the centre along its entire length. Extreme care was taken not to disturb the fibre or add any air bubbles. The moulds containing the fibre and the epoxy were kept in the oven and cured at 80 °C for 3 h. After the curing time, the oven was turned off and the specimens were allowed to cool slowly to reduce the residual stresses.

The cured SFC specimens were polished using metallographic polishing wheels. The specimens thus obtained were transparent and suitable for optical microscopy. To avoid the effects due to physical ageing of the matrix, the SFC tests were conducted within 3 days after fabricating the specimens. Before testing, the SFC specimens were inspected for defects, such as air bubbles and the defective specimens were discarded.

The SFC specimens were strained uniaxially using a small strain frame. An Olympus model PME light microscope with polarizer attachment was used to observe the fibre fragmentation. The specimen, with a gauge length of 20 mm, was mounted on the strain frame and strained in small steps of about 0.2% strain. The $X-Y$ stage controls allowed the observation of the entire specimen gauge length. After each strain increment, the entire specimen was scanned to locate the fibre breaks. In this manner, the entire progression of fibre breaks was monitored. At the end of the test, the fracture locations, and fragment lengths could be measured using a calibrated eye piece. A total of six SFC specimens were studied. From the measured strain of the specimen at each fibre fracture, the fibre strength values were estimated by multiplying the corresponding strains by the fibre modulus of 176.4 GPa. It was thus assumed that the fibre strain was the same as the specimen strain. This assumption is reasonable because we did not see significant gaps between the two fragment ends during the SFC tests.

A torque meter was attached to the strain frame to obtain consistent starting (zero strain) point. This was necessary because of the critical nature of the strain measurement and the possibility of some specimens being mounted with a small amount of slack. Birefringence patterns around the fibre breaks were observed to assess the extent of debonding and to ensure that no matrix cracking occurred.

4. Results and discussion

Fig. 3 shows the typical Weibull plot for the SFC specimen 5 in terms of fibre fracture strength versus fracture probability. The smallest fragment length in this specimen was 0.7 mm, so the SFC specimen was assumed to be partitioned into 29 short sections. Because 19 of them contained fibre fracture points, the strength data for these 19 sections are plotted as the censored data on the Weibull probability paper. It can be seen that the plot looks like a straight line indicating a good fit of the data to the Weibull distribution. Several specimens showed similar behaviour, i.e. a straight line, but some other specimens tended to show a bilinear behaviour, indicating a bimodal distribution [22, 24]. The property of this bimodality is discussed later.

Fig. 4 shows the relation between the estimated values of the Weibull shape parameter and the

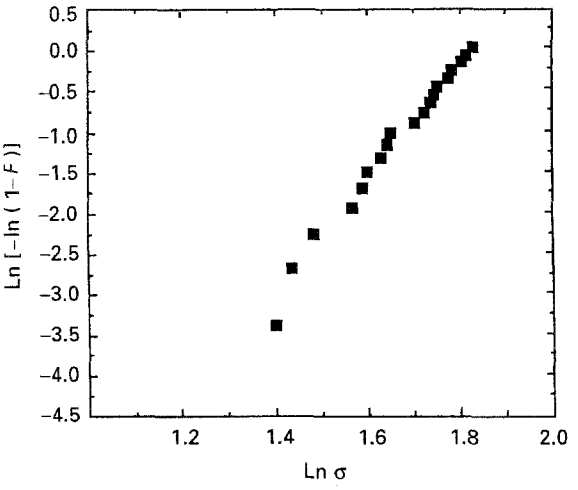

Figure 3 Typical Weibull plot for the SFC specimen 5 in terms of fracture strength versus fracture probability.

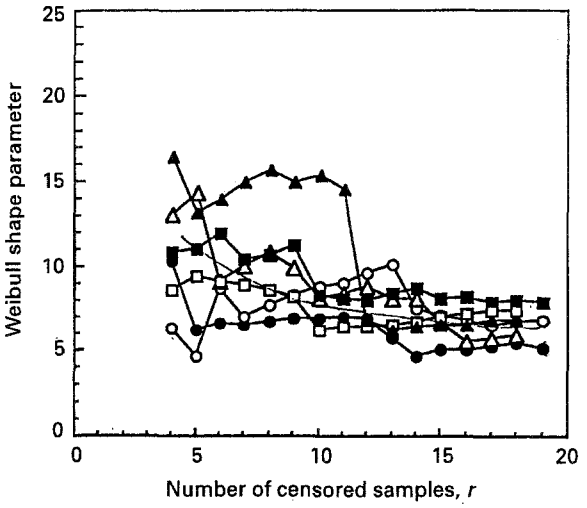

Figure 4 Relation between the estimators of the Weibull shape parameter and the number of the censored samples: (●) 1, (○) 2, (△) 3, (■) 4, (□) 5, (▲) 6.

TABLE I Average strength and Weibull parameters of Nicalon™ fibre

Gauge length (mm)	Mean strength (MPa)	Scale parameter (MPa)	Shape parameter
5[a]	3265	3639	3.36
10	3194	3479	4.80
100[a]	2263	2511	3.52
200	1872	2027	5.55

[a]Values obtained from [15].

number of the censored sample. The estimators, e.g. for $r = 4$, means that the fourth fibre fracture strength value was chosen as the last censored datum, σ_r, i.e. only the first four data (fracture) points were used in the estimation, in spite of the fact that the total censored data are 18–19. The Weibull shape parameters for all six specimens start between 7 and 16 and gradually decrease with the number of censored samples and finally settle between 5.2 and 8.8. It is known that a smaller number of samples generally produces higher value for the shape parameter than for a larger sample size, because of the biased property, of the maximum likelihood estimation method [23]. The data presented in Fig. 4 support this argument.

In Table I, we show the Weibull scale and shape parameters as well as the mean values for the strength of Nicalon™ fibres as a function of the gauge length (size effect) obtained from the tension tests. The shape parameter estimated by the SFC method is higher than that obtained by the conventional single fibre tension tests carried at 10 mm gauge length. There may be two reasons for this difference. First, in the SFC test method, only a single fibre is tested. As a result of this, the effect of variability among fibres is not included as is the case with the tension tests. Another reason is that the Nicalon™ fibre has been shown to have two types of flaws that result in a bimodal strength distribution depending on the flaw types [22]. One of them is a surface flaw such as a "pit", and the other one is an internal flaw such as a "void". The internal defects were related to the strength at short gauge lengths, and tended to give higher shape parameter values [22]. In other words, the surface flaws govern the initial fibre fracture while the internal defects govern the latter part of the fracture process during the SFC test when the fragment lengths become very short. Sachse *et al.* [15] who studied fibre strength using the acoustic emission-coupled SFC technique also reported two flaw populations for similar Nicalon™ fibres. The bimodality of the strength distribution, dependent on the two types of defects, appears not only in Nicalon™ fibres but also in several other reinforcing ceramic fibres, such as carbon [25], boron [26] and glass [27]. Therefore, in general, the shape parameter values in the SFC test are expected to be larger.

Fig. 5 shows the change in the estimated values of the Weibull scale parameter extrapolated to the gauge length of 10 mm, with the number of the censored sample. The estimates are in the range of 4.0–4.6 GPa,

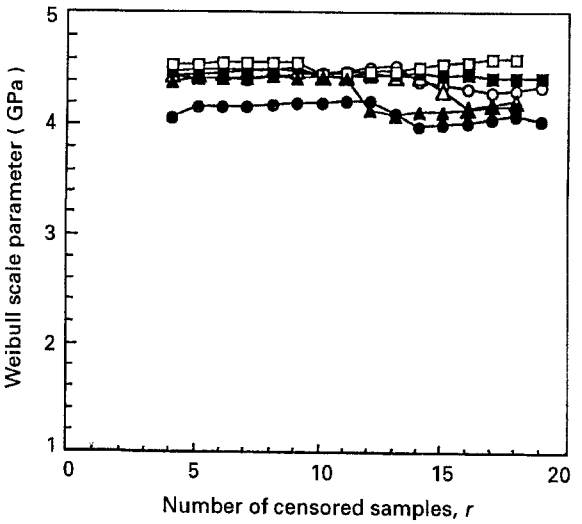

Figure 5 Relation between the estimators of the Weibull scale parameter and the number of the censored samples. For key, see Fig. 4.

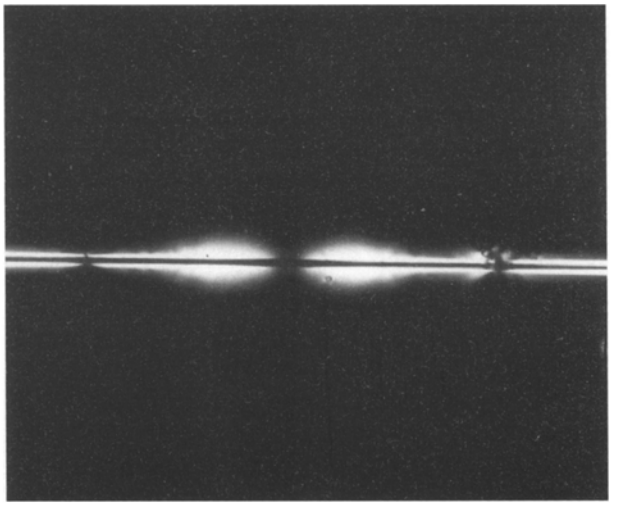

Figure 6 A typical optical photomicrograph showing the birefringence pattern around a fibre fracture.

independent of the number of the censored sample. These values again are higher than the results obtained from the single-filament tension tests shown in Table I. There are several reasons for this discrepancy. One reason is that the "effective" gauge length in the SFC experiment is shorter than the actual gauge length, because of the extensive fibre/matrix debonding occurring around the fibre fracture locations. Fig. 6 shows a typical optical micrograph of the birefringence pattern around a fibre fracture. The nodes away from the fracture point indicate an unfailed interface while the distance from the fracture point to the nodes on either side, is the debonded interface. The lengths of the debonded regions are known to increase with strain in tension, and complicate the stress field as fracture points accumulate [3]. Fig. 7 shows the schematic illustration of the stress profile and the bilinear stress recovery regions between the fracture points. The "effective" gauge length is taken as the fragment length from one fracture point to the next minus the stress recovery regions on both sides, length CD in Fig. 7. The "effective" gauge length is a function

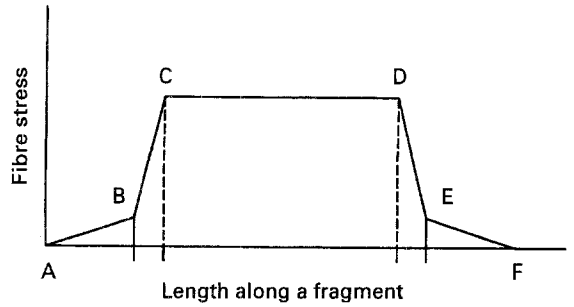

Figure 7 Schematic illustration of the bilinear stress profile between the fracture points in the SFC specimen. AF, fragment gauge length; AB, FE, fibre/matrix friction (debonded region); BC, DE, fibre/matrix shear (bonded region); CD, effective fragment gauge length; AC, ineffective length.

of strain, and decreases as the debond regions grow with strain as shown by the regions AB and EF in Fig. 7. Therefore, "effective" lengths were also given to the length L_0 of the individual short sections, and the length L_0 became shorter than 0.7 mm used in this analysis. Consequently, the scale parameters obtained by the SFC test are higher than that obtained by the single-fibre tension test. Also, as mentioned earlier, the fragments are not subjected to full load within the stress recovery regions (BC and DE) and hence, the defects present in these regions are not detected, contributing to the higher scale parameter.

Another reason why the values obtained for the scale parameters are different in the present method is the significant difference between the coefficients of thermal expansion (CTE) of the Nicalon™ fibre and the epoxy matrix used in this study. The shrinkage of the epoxy matrix is higher than that of the Nicalon™ fibre, when cooled to room temperature after curing at elevated temperature. This differential shrinkage generates compressive residual stress on the fibres. During the SFC test, the initial part of the strain is used in removing the residual stress. The rest of the strain contributes to the tensile stress on the fibre. The residual stresses can generally be estimated by taking a one-dimensional equilibrium equation as follows [19]

$$\sigma_{\text{resid}} = (\alpha_{\text{epoxy}} - \alpha_{\text{Nic}})\Delta T E(\varepsilon) \quad (7)$$

where $E(\varepsilon)$ is the modulus of the measured stress/strain response of the specimen and α is the CTE. The CTE of epoxy is $30 \times 10^{-6}\,^{\circ}\text{C}^{-1}$ at 80 °C, and the CTE of Nicalon™ fibre is $4 \times 10^{-6}\,^{\circ}\text{C}^{-1}$. Measured average values for $\alpha_{\text{epoxy}}\,\Delta T$ for the epoxy was about 0.25%. On the other hand, this quantity for the fibre is much smaller and may be neglected. The curing at 80 °C yields a shrinkage strain of 0.25%. Using Equation 7 the residual tensile stress value for Nicalon™ fibre was calculated to be 440 MPa. This value was applied as the correction of the scale parameter estimated by the SFC test, as described later.

The value 3479 MPa of the scale parameter estimated from the SFC test also needs a correction to account for the smaller "effective" gauge length. From our experiments we estimated that approximately one-third of the fragment length was debonded so that

TABLE II Comparison of scale parameters from the two tests

Tension test (MPa)	SFC test (MPa)
3479 for 10 mm 3788 for 6.7 mm[a]	4288 for 6.7 mm – 440 for shrinkage
Final 3788	3888

[a]Value calculated using Equation 8.

the corrected length is equivalent to 6.7 mm. Sachse *et al.* [15] determined roughly the same ratio of the debond length to the gauge length of several SFC specimens by acoustic emission (AE)-coupled SFC technique. Therefore, for comparison, the scale parameter obtained for the gauge length of 10 mm by tension test can be scaled to a length of 6.7 mm, for comparing with that obtained by SFC technique, by using the Weibull weakest link rule as follows

$$\sigma_{6.7} = \sigma_{10}(L_{6.7}/L_{10})^{-1/\rho} \quad (8)$$

By taking into account the residual stress and the debonding length in the SFC specimen, the scale parameters obtained from SFC test were corrected. The result showed that both values are in good agreement, as indicated in Table II.

5. Conclusions

It has been shown that the new theory described here, can be used to obtain good estimate of the Weibull shape and scale parameters for the *in situ* fibre strength. Although there exists a good agreement between the strength values obtained by the new technique and the single filament tension test, the values from SFC are expected to be higher because of several reasons mentioned above. Because the environment around the fibre in the SFC specimens is closer to that of the fibres in actual composites, the strength values obtained by the present method may be of more practical importance than those obtained by the single filament tension tests for the evaluation of composites.

References

1. L. T. DRZAL, M. J. RICH, M. E. KOENIG and P. F. LLOYD, *J. Adhes.* **16** (1983) 133.
2. W. D. BASCOM and R. M. JENSEN, *ibid.* **19** (1986) 219.
3. A. N. NETRAVALI, R. B. HENSTENBURG, S. L. PHOENIX and P. SCHWARTZ, *Polym. Compos.* **10** (1989) 226.
4. S. H. OWN, R. V. SUBRAMANIAN and S. C. SAUNDERS, *J. Mater. Sci.* **21** (1986) 3912.
5. A. N. NETRAVALI, Z.-F. LI, W. SACHSE and H. F. WU, *ibid.* **26** (1991) 6631.
6. A. N. NETRAVALI, S. L. PHOENIX and P. SCHWARTZ, *Polym. Compos.* **10** (1989) 385.
7. A. S. WIMOLKIATISAK and J. P. BELL, *ibid.* **10** (1989) 162.
8. W. A. CURTIN, *J. Mater. Sci.* **26** (1991) 5239.
9. M. R. PIGGOTT and Z. N. WANG, in "Proceedings of the 6th Technical Conference of the American Society for Composites", Albany, NY (Technomic, 1991) pp. 725–31.
10. L. S. PENN and S. M. LEE, *J. Compos. Tech. Tech. Res.* **11** (1989) 23.

11. U. GAUR, C. T. CHOU and B. MILLER, in"Proceedings of the 6th Technical Conference of the American Society for Composites", Albany, NY (Technomic, 1991) pp. 751–58.
12. Y. QIU and P. SCHWARTZ, *J. Adhes. Sci. Tech.* **5** (1991) 741.
13. H. D. WAGNER and A. EITAN, *Appl. Phys. Lett.* **56** (1990) 1965.
14. B. YAVIN, H. E. GALLIS, J. SCHERF, A. EITAN and H. D. WAGNER, *Polym. Compos.* **12** (1991) 436.
15. W. SACHSE, A. N. NETRAVALI and A. R. BAKER, *J. Nondestruc. Eval.* **11** (1993) 251.
16. M. C. WATERBURY and L. T. DRZAL, *J. Compos. Test. Tech. Res.* **13** (1991) 22.
17. R. B. HENSTENBURG and S. L. PHOENIX, *Polym. Compos.* **10** (1989) 389.
18. A. KELLY and W. R. TYSON, *J. Mech. Phys. Solids* **13** (1965) 329.
19. A. KELLY, *Proc. R. Soc. Lond.* **A 319** (1970) 95.
20. H. F. WU and A. N. NETRAVALI, *J. Mater. Sci.* **27** (1992) 3318.
21. A. C. COHEN, *Technometrics* **7** (1965) 579.
22. K. GODA and H. FUKUNAGA, *J. Mater. Sci.* **21** (1986) 4475.
23. G. SIMON and A. R. BUNSELL, *ibid.* **19** (1984) 3649.
24. D. R. THOMAN, L. J. BAIN and C. E. ANTLE, *Technometrics* **11** (1969) 445.
25. C. P. BEETZ JR, *Fibre Sci. Technol.* **16** (1982) 45.
26. G. K. LAYDEN, *J. Mater. Sci.* **8** (1973) 1581.
27. A. G. METCALFE and G. K. SCHMITZ, in "Proceedings of the 67th Meeting of the ASTM (American Society for Testing and Materials, Philadelphia, PA, 1964) pp. 1075–93.

Received 23 June 1993
and accepted 8 September 1994